ELSEVIER

Biochimica et Biophysica Acta 1273 (1996) 139–149

BBA Biochimica et Biophysica Acta

Intramembrane electron transfer: processes in the photosynthetic reaction center

Lev I. Krishtalik *

A.N. Frumkin Institute of Electrochemistry, Russian Academy of Sciences, Leninskii prosp. 31, 117071 Moscow, Russia

Received 3 April 1995; revised 30 August 1995; accepted 3 October 1995

Abstract

The intramembrane charge transfer has been analyzed in the framework of the 'fixed-charge-density' formalism. For a three-layer model of membrane, the expressions for the reorganization energy have been derived. In the case of very fast reactions, the time-evolution of the dielectric response of a protein should be taken into account. This has been described phenomenologically in terms of a set of effective dielectric constants, ε_T, operative in different time intervals. For the charge separation process, the effects of the variable ε_T on the reaction free energy and on the medium reorganization energy are equal and opposite in sign, and hence compensate each other. As a result, the photosynthetic primary charge separation proves to be activationless, irrespective of the value of ε_T. On the basis of the existing experimental data, the semiquantitative estimates of ε_T at different times were given. With these values of ε_T, the activation energy close to zero was calculated for the reactions of electron transfer from bacteriopheophytin to quinone, of recombination of the primary radical-ion pair with formation of a neutral triplet, and of recombination of the special pair cation with quinone anion.

Keywords: Photosynthesis; Electron transfer; Charge separation; Dielectric relaxation; Protein relaxation; Protein as a dielectric

1. Introduction

Intramembrane electron transfer is one of the most common and important processes in bioenergetics. Many of these reactions are very fast, the fastest of them, viz. the primary charge separation in photosynthetic reaction centers (RC), having a characteristic duration of a few picoseconds. The upper limit of the reaction rate is achieved due to the activationless character of the process [1–4].

The activation energy of the elementary act of electron transfer $E^{\neq}$ is determined, according to a well-known equation, by two parameters, namely the reorganization energy, E_r, and the free energy of the reaction, ΔG

$$E^{\neq} = \frac{(E_r + \Delta G)^2}{4E_r} \tag{1}$$

The reorganization energy, E_r, can be considered as the sum of the inner-sphere E_i and medium E_s contributions. The activation energy reaches zero when the reorganization energy, E_r, equals the negative value of the reaction free energy, ΔG. Even in the case that this equality holds true only approximately, with the sum $E_r + \Delta G < kT$, the process behaves practically as an activationless one.

Electron transfers in biological membranes take place inside special protein complexes, and hence their characteristics are affected substantially by the properties of these proteins. The specific features of proteins are their relatively low static dielectric constants resulting in low reorganization energies, and the existence of a permanent intraprotein electric field influencing markedly the reaction free energy (for reviews see [5–7]).

For very fast reactions, a new factor, specific of proteins, enters the scenario, namely a wide distribution of characteristic times of their dielectric responses. In proteins, a hierarchy of different motions exists, with their characteristic times lying in the interval of several orders of magnitude wide [8–11]. Evidently, for very short reaction times, some kinds of relatively slow polarization modes do not have enough time to manifest themselves in the course of the charge transfer, and hence the effective medium dielectric response is lower than the static dielectric constant.

Abbreviations: *Rb.*, *Rhodobacter*; *Rps.*, *Rhodopseudomonas*; RC, reaction center; P, special pair (bacteriochlorophyll dimer); P^*, the special pair in the excited state; BPh, bacteriopheophytin; BChl, auxiliary bacteriochlorophyll; Q_A, Q_B, quinones in branches A and B.

* Corresponding author. Fax: +7 095 9520846.

0005-2728/96/$15.00
SSDI 0005-2728(95)00135-2

This problem has been analyzed in my previous paper [12] in terms of a set of effective dielectric constants, ε_T, operative in corresponding time intervals. It was concluded that the primary charge separation process in photosynthetic RC is activationless irrespective of the temporary value of ε_T. It was shown also that the effective ε_T are substantially different for different time intervals characteristic of the processes in RC.

The drawback of my previous analysis was that it employed formulae [13] derived on a not quite rigorous basis. In fact, two different approaches to calculations of the reorganization energy were used in the literature. They gave coinciding results for homogeneous, but quantitatively different ones for nonhomogeneous media. These approaches can be called 'fixed-displacement-field' and 'fixed-charge-density' methods [14]. In my previous work [13], I have used the first technique. However, quite recently, convincing arguments in favor of the 'fixed-charge-density' formalism as the only rigorous one have been given [14–16]. That means that, to obtain the reorganization energy, the general equation, Eq. (2), should be used:

$$E_s = \frac{1}{8\pi}\int_V\left[\frac{1}{\varepsilon_0}(\mathbf{D}_i^o - \mathbf{D}_f^o)^2 - \frac{1}{\varepsilon_s}(\mathbf{D}_i^s - \mathbf{D}_f^s)^2\right]dv \qquad (2)$$

Here, ε_0 and ε_s are optical and static dielectric constants, $\mathbf{D}_i$ and $\mathbf{D}_f$ are the electric displacement vectors corresponding to initial and final charge distribution, $\mathbf{D}^o$ and $\mathbf{D}^s$ are calculated under conditions where all dielectric phases have their optical or, correspondingly, static ε's. The integration is extended over the total system volume V, except for the volume of the reactants.

On the basis of Eq. (2), I have derived an expression for the medium reorganization energy employing the three-layer model of a membrane system [17] (for some details, see Appendix B). Using this formula, we have calculated the reorganization energies for different intramembrane electron transfer reactions under various conditions. The results of these calculations are presented below; they confirm in a general outline the principal conclusions of the previous paper [12] that were obtained in a less rigorous way. In addition, the analysis was extended to some reactions that were not discussed in [12] (some parts of Sections 3 and 5).

2. Charge separation process: a general analysis

As in [12], we will consider the problem phenomenologically, describing the protein as a dielectric medium having a set of different dielectric constants ε_T operative in different time intervals: in some short time span, only librations and bendings of some side-chain polar groups contribute substantially to polarization fluctuations, at longer times the movement of other dipoles, including a part of the backbone peptide groups, gives an additional effect, etc. Thus, ε_T reflects not only the electronic polarization (as optical ε_0 does) but also some part of inertial polarization due to the shift of nuclei; therefore, it can be called the 'quasi-static' constant. We will consider here only the influence of this relaxation times distribution on the activation energy, and not on the pre-exponential factor; the latter effect should be expected in the specific case of the reaction time close to one of the dielectric relaxation times (see, for example, [18,19] and references therein).

As ε_T is time-dependent, all the energies (e.g., of solvation, interaction, reorganization) are also functions of time.

The reaction free energy can be represented as the sum of some 'inner', quantum-chemical contribution determined by the reactants' structures, ΔG_{st}, and some electrostatic charging energy, ΔG_{el}, which is the sum of the energies of charging of the reactants when they are separated and the energy of their interaction at given positions in the medium of dielectric constant ε_T. [1]

In my previous paper [12] I have shown that, in the model of an infinite homogeneous dielectric, the sum of reorganization energy and the electrostatic component of reaction energy is independent of the value of ε_T: the effects of the variable ε_T upon the reaction energy and the reorganization energy are equal and opposite in sign, and, therefore, are strictly compensating each other.

Using the 'fixed-charge-density' formalism it becomes possible now to show quite strictly that the sum $E_r + \Delta G_{el}$ for the charge separation process is independent of ε_T in any inhomogeneous medium (including the inhomogeneity due to the presence of the second reactant, the effect of which was neglected in the previous analysis).

For the charging energy of the system of two initially neutral particles we can write a quite general expression

$$E_{ch} = \frac{1}{8\pi}\int_V \frac{1}{\varepsilon_s}(\mathbf{D}_f^s)^2 dv \qquad (3)$$

Note that the initial $\mathbf{D}_i^s = 0$ because both particles in this state are neutral. The displacement $\mathbf{D}_f$ is a superposition of fields of two ions having charges $+e$ and $-e$

$$\mathbf{D}_f = f_1 e - f_2 e \qquad (4)$$

where f_1 and f_2 are functions of a quite general form describing the field in any point and depending on location of ions, the charge density distribution inside them, and the geometry and dielectric properties of the system. For our

---

[1] The structure-dependent component includes the effect of an external (relative to reacting molecules) electric field set up by the fixed permanent dipoles of the protein; this item depends on the protein structure [5–7]. The dipoles' field existed long before the appearance of the newly-formed charges, and hence it does not depend on the variable constant ε_T. In contrast, the total charging energy, ΔG_{el}, is determined by the variable ε_T which describes the additional polarization evolving in time after the charge transfer [12].

purpose, it is important only that the field is proportional to the charges of the ions.

From Eqs. (3) and (4) we have

$$E_{\text{ch}} = \frac{1}{8\pi} \int_V \frac{e^2}{\varepsilon_s} (f_1^2 + f_2^2 - 2f_1 f_2) \mathrm{d}V \qquad (5)$$

If we turn now to the second term of the general expression for E_s, i.e., Eq. (2), and substitute zero for $\mathbf{D}_i^s$ and Eq. (4) for $\mathbf{D}_f^s$, we obtain the same expression (5) but with the sign minus.

These considerations show that the mutual compensation of the equilibrium electrostatic energy and of the ε_s-dependent part of the reorganization energy is a quite general feature of the charge separation process, and this result holds true at any geometry of the system. Earlier, I considered this result a good approximation obtained for my membrane model [12]. I see now that in the more rigorous 'fixed-charge' formalism this is an exact result.

The compensation of the ε_s-dependent components of reorganization and reaction energies is an intrinsic property of the charge separation only, and it does not take place for other charge transfer processes (see Appendix A).

The exact compensation of effects of ε_T on E_s and ΔG_{el} means that if it is shown that $E_r = -\Delta G_{\text{cs}}$ at any particular value of ε_T (here ΔG_{cs} is the total ΔG of the charge separation), i.e., the process is activationless under these conditions, it will remain activationless at any other ε_T, i.e., at any moment of the time-evolution of the dielectric response.

3. Primary charge separation in RC

Let us consider, in the framework of the general approach outlined in the previous section, the process of primary charge separation in the RC. To find out whether the reaction is really activationless, we have to compare two quantities: ΔG and E_r. In the following, I will use the experimental estimates of ΔG at different time intervals and the corresponding E_r values calculated theoretically.

For the components of photosynthetic RC, the inner-sphere contributions to E_r are small; the estimate for chlorophylls gives a practically vanishing E_i [20], for quinones $E_i \approx 0.04$ eV [21,22]. It should be noted that this component relates to the molecular distortions of a higher frequency, and hence its influence on the classical reorganization energy may manifest itself in a not full extent.

The medium reorganization energy, E_s, was calculated by the formulae given in Appendix B. They were derived in the framework of the three-layer model proposed earlier [17]. This model takes into account the different dielectric properties of the membrane's low-polar inner core (hydrocarbon chains of lipids, α-helical segments of the hydrophobic intramembrane proteins) and of the membrane's outer layers of intermediate polarity (lipid polar heads, hydrophilic segments of proteins). The different dielectric constants of inner and outer parts of a photosynthetic membrane reveal themselves in the magnitudes of electrogenic effects in these membranes [23]. The model supposes sharp boundaries between dielectric layers and, therefore, has a somewhat conditional character because one should expect more probably a smooth change of dielectric constant along the normal to the surface. Nevertheless, in absence of any experimental data on the spatial distribution of ε, I prefer to use a stepwise model function to obtain a reasonable estimate of the effects due to medium inhomogeneity.

The geometric parameters of membrane and the disposition of the reactants inside it were estimated as in [12] (the data are summarized in Appendix C).

The value of ε_o for the inner layer was accepted to be 2.5. The optical dielectric constant of amides is 2.1 to 2.2, but we have to include in the effective value of ε_o not only electronic polarization but also the polarization components due to fast, high-frequency quantum modes like, for example, N–H vibrations [24,25]. For water, this effect increases 'quantum' ε from $\varepsilon_o = 1.8$ to approx. 2.1 [24], a similar (but a little bit smaller in percentage) effect we have accepted for protein. The intermediate layer contains, beside the protein, a marked amount of water; therefore, a somewhat lower value of $\varepsilon_o \approx 2.3$ to 2.4 was ascribed to this layer. Its decrease increases E_s by only 3 meV. Similar variations in ε_o of the outer aqueous surroundings result in shifts of about 0.5 meV.

The quasi-static ε_T of the inner core was varied from 2.6 to 4. For the intermediate layer that, in the vicinity of RC, is proteinaceous, it is reasonable to suppose approximately the same relaxation kinetics as for the intramembrane protein. Hence, I accepted its ε_T permanently 4-times larger than ε_T of the inner core; the ratio of 4 or somewhat larger was deduced in [17] on the basis of the data on electrogenic effects. Due to a very fast relaxation of water (the longitudinal dielectric relaxation time lies in picosecond range), I have accepted ε_T for aqueous surroundings to be equal to the stationary value, viz. 78.

Some typical results of calculations for the electron transfer $P^* \rightarrow$ BPh are presented in Fig. 1 as a function of ε_T. Curve 1 shows the component analogous to the reorganization energy in an infinite homogeneous dielectric (Marcus Eq. (AII.4), i.e., Eq. (AII.2) and three first terms of Eq. (AII.3) in Appendix B). This part depends markedly on the value of the optical (quantum) dielectric constant ε_0. For instance, if I were to accept instead of $\varepsilon_0 = 2.5$ the value $\varepsilon_0 = 2.4$, the reorganization energy would increase by 24 meV.

Curve 2 presents the component due to the effect of image charges (the solution of the electrostatic problem in form of series of image charges is described in App. A). This contribution decreases with increasing ε_T, compensating partly the increase in the first component (Curve 1). The decrease in the image-charges contribution steepens as

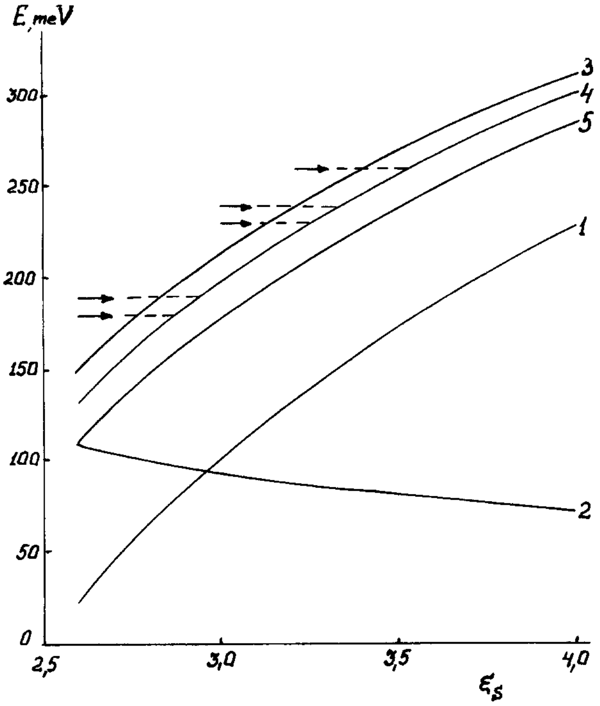

Fig. 1. The components of reorganization energy as a function of the effective dielectric constant ε_T. Curve 1 – according to Marcus formula for an infinite medium, Eq. (AII.4); 2 – component due to effect of images, 3–5 – total reorganization energy, all calculated with Eqs. (AII.2, 3). The distance between the center of the special pair P and the closest boundary of phases I and II equals 0.45 nm (Curve 3), 0.5 nm (4), 0.6 nm (5). The other parameters as described in the text and Appendix C.

the reactants approach the membrane boundaries, i.e., as they approach the first image. The image effect is proportional to the difference of dielectric constants of two media. Therefore, the contribution of charging in the optical-dielectric-constant medium is small (e.g., about 5 meV) and practically insensitive to the value of ε_0; for instance, substitution of $\varepsilon_0 = 2.4$ for 2.5 increases it only by 0.4 meV.

Curves 3–5 give the total reorganization energy [2] for three different distances of P to the closest boundary. Variation of the latter parameter within reasonable bounds gives a rather small but nevertheless perceptible effect of 0.01 to 0.02 eV.

Let us compare these results with the experimental data on the energy gap for this reaction. From the data on delayed fluorescence in RC of *Rb. sphaeroides*, the initial (in the time range of picoseconds) ΔG_{cs} for the primary charge separation was estimated to be −0.16 eV in the presence of Q_A^- [26] and −0.18 to −0.19 eV in its absence [27]. After 10 ns the gap increases to −0.21 eV and −0.23 to −0.24 eV, respectively. A much lower initial value of about −0.08 eV and very close to that given above at 10 ns (−0.20 eV, in the presence of Q_A^-) were obtained recently [28] (cf. also the results of [29]). The experiments on the triplet decay rate (timescale about 100 μs) give $\Delta G_{cs} = -0.26$ eV [30]. For the RC of *Rps. viridis*, in the time interval of few milliseconds, $\Delta G_{cs} = -0.30$ eV was obtained [31]. The equilibrium value −0.34 eV deduced for this object [27] is, probably, somewhat influenced by additional relaxation processes, and is possibly not purely dielectric by nature (see below, Section 4); therefore, we can accept for $\varepsilon_s = 4$ a value of $\Delta G_{cs} \approx -0.30$ to −0.32 eV.

At the stationary $\varepsilon_T = \varepsilon_s = 4$, I calculated the reorganization energy $E_s = 0.30 \pm 0.01$ eV. This value practically coincides with the experimental $-\Delta G \approx 0.30$ to 0.32 eV. That shows that the charge separation process should be activationless. This conclusion holds practically true even at a markedly larger difference of E_s and $-\Delta G$; e.g., at $E_s + \Delta G = 0.05$ eV (which exceeds the probable scatter of the computed quantities), the activation energy should be equal to 0.002 eV, and the reaction would be practically indiscernible from the activationless one. Therefore, we can conclude that the possible inaccuracy in the estimation of the parameters cannot change the principal conclusion on the practically activationless character of the reaction.

The above calculations relate to the stationary value of $\varepsilon_s = 4$. However, as we have shown in the previous section, the final result, viz. the activation energy close to zero, holds true independently of the time evolution of the medium dielectric response. The conclusion on the activationless character of the primary charge separation has been obtained without resorting to any adjustable parameter.

It should be noted that the total dielectric constant may change not only as a result of the temporal evolution of polarization but also under the influence of other factors, first of all the temperature. However, these variations will again exert an effect equal and opposite in sign on both E_s and ΔG_{cs}^o, these shifts exactly compensating each other, and the process retains its activationless character at other temperatures, too [12]. The change of ΔG_{cs}^o with temperature has been discussed many times (see, for example, [28,29] and the literature quoted therein). The possibility of a substantial temperature dependence of E_s was stressed in [32]. Important is that these changes are parallel and compensate each other.

A substantial decrease in ε_s at low temperatures is due to the 'freezing-out' of some high-frequency polarization modes; at these temperatures, their contribution should be treated quantum-mechanically [2,3,5,25]. An additional difficulty in the theoretical treatment of the low-temperature data is related to the substantially nonequilibrium character of the reactants' surroundings. It is highly probable that, after the sample freezing, many dipoles turned to be fixed in positions that were easy to obtain at high

---

[2] The results of these calculations are quantitatively quite close to the previous ones [12]. This is due to the fact that the main terms in Eqs. (AII.2,3) and in the incorrect equation from [13] are identical, and the other terms, in our particular case, are small.

temperatures but are practically inaccessible by equilibrium low-temperature fluctuations. This results in a substantial 'biographical' inhomogeneity of the reactants' surroundings.

As was described above, the experimental values of ΔG_{cs} depend strongly on the time interval characteristic of the measurement method. This effect was explained qualitatively by Woodbury and Parson [26] and Bixon and Jortner [33] as a result of stabilization of charged state due to a gradual development in time of the protein dielectric polarization. This concept of 'dynamic solvation' was employed recently by Peloquin, Woodbury et al. [28,29] as well as in my previous paper [12] [3]. An alternative explanation of the multiexponential kinetics in the RC spectral properties, namely a substantial inhomogeneity of RC's, has been proposed many times (see, for example, the literature quoted in [28,29]), and has been advocated especially in the recent paper by Ogrodnik et al. [35]. It seems quite probable that the inhomogeneity plays an important role during the short initial periods, but it can hardly explain fully the behavior in the time intervals of tens of nanoseconds [28,29] and, especially, at much longer times. It should be noted here that both the set of different (in time and magnitude) dielectric responses and the energetic inhomogeneity have a common physical origin. This is the existence in proteins of substantially different kinds of motion that should reveal themselves at higher temperatures mostly as a time-evolution of the dielectric response, and at low temperatures as a well-expressed biographical inhomogeneity. Taking into account these considerations, I will describe the time dependence of the experimental ΔG_{cs} at physiological temperatures as due mainly to the time-evolution of the effective dielectric constant.

The values of ΔG_{cs} are shown by arrows in Fig. 1. We see that for $\Delta G_{cs} = -0.18$ to -0.19 eV observed in the picosecond time span [4], $E_s = -\Delta G_{cs}$ at $\varepsilon_T \approx 2.9$; for the interval of 10 ns we obtain $\varepsilon_T \approx 3.3$, for 100 μs $\varepsilon_T \approx 3.5$. The dependence of E_s on ε_T is due to the influence of ε_T on the total charging energy, and the effect, as was stressed before, is the same for E_s and $-\Delta G_{cs}$. Therefore, the effective values of ε_T estimated above are not dependent on the condition $E_s = -\Delta G_{cs}$ but are a direct consequence of the ε_T-dependence of ΔG_{cs}. Indeed, if we accept the equilibrium value of $\Delta G_{cs} = -0.30$ eV at stationary $\varepsilon_s = 4$, then $\Delta G_{cs} = -0.18$ to -0.19 eV corresponds to $\varepsilon_T \approx 2.88$ to 2.95, $\Delta G_{cs} = -0.23$ to -0.24 eV to $\varepsilon_T \approx 3.26$ to 3.34, and $\Delta G_{cs} = -0.26$ eV to $\varepsilon_T \approx 3.55$ (see, for example, curve 4). If we accept the value $\Delta G_{cs} = -0.31$ eV at $\varepsilon_s = 4$, then the corresponding ε_T values would be 2.78–2.84; 3.15–3.23; 3.41 (curve 3), etc. These variable values I will use in my subsequent discussions. As the curves 3–5 are almost parallel, the estimated effective ε_T values are only slightly sensitive to geometric parameters of the model; of principal importance is the difference between the steady-state and temporal values of ΔG_{cs}.

The main conclusion following from this analysis is that the effective dielectric constant, more exactly its inertial component, is subject to an essential time evolution.

Let us compare now the continuum calculations with a molecular dynamic analysis [36–39]. The latter relates to the short time spans, namely up to about 20 ps. The computed reorganization energies match quite well the energy $\Delta G_{cs} = -0.18$ to -0.19 eV characteristic of this time interval. The same result, viz. practically coinciding $-\Delta G_{cs}$ and E_s, was obtained by the longest-lasting (60 ps) simulation in [40].

Until now, I have considered the reaction $P^* \rightarrow BPh$ as a single act, with the auxiliary BChl serving only as a bridge assisting electron transfer. The other possibility has been supposed, namely that the process proceeds in two steps with an intermediate formation of $BChl^-$ [41,42]. I am not going to discuss this complicated problem in detail here; nevertheless, it seems useful to list some estimates of the energetics of this two-step mechanism.

I have calculated reorganization energies for $P^* \rightarrow BChl$ and $BChl^- \rightarrow BPh$ electron transfers using a ε_T characteristic of a picosecond interval (2.8 to 2.9). For the first step it is 0.11–0.12 eV, for the second one 0.08–0.10 eV. There are no accurate data on the ΔG of these processes. Two different estimates were considered: $\Delta G_1 \approx 0$, $\Delta G_2 \approx \Delta G_{cs} = -0.18$ eV [43] and $\Delta G_1 \approx \Delta G_{cs}$, $\Delta G_2 \approx 0$ [41]. For the first version, $E_1^{\neq} = 27$–30 meV, $E_2^{\neq} = 16$–31 meV (the second step lies in the inverted region); the second version gives $E_1^{\neq} = 8$–11 meV, $E_2^{\neq} = 20$–25 meV (first step in the inverted region). The first version does not match the activationless character of the process very well. The situation for the second version is a little better. However, all the barriers given above are rather low, and, moreover, they can be surmounted, as was supposed in [22], at the expense of the nonequilibrium excess energy stored at a vertical Franck-Condon transition in the excited state P^*. In the process with this nonequilibrium energy employed, the thermal fluctuations are unnecessary, and hence no activation energy should be observed.

The results of these calculations are rather sensitive to the choice of ΔG value. If the $BChl^-$ level lies a little bit higher than that of P^*, the activation energy becomes substantial, e.g., at $\Delta G_1 = +0.05$ eV ($\Delta G_2 = -0.23$ eV), $E_1^{\neq} = 58$–60 meV, $E_2^{\neq} = 42$–70 meV. The situation will improve markedly should the energy level of the intermediate state lie between the levels of P^* and BPh^-, preferably closer to the latter. For instance, with $\Delta G_1 = -0.12$ eV and $\Delta G_2 = -0.06$ eV we obtain $E_1^{\neq} = 0.0$–0.2 meV and $E_2^{\neq} = 1.2$–4.0 meV.

---

[3] The time evolution of the protein dielectric response has been inferred also from the shift of the fluorescence spectra of some dye-protein complexes ([34]; Mertz, E.L. and Krishtalik, L.I., unpublished result).

[4] The lower ΔG_{cs} observed at the shortest times [28] correspond to $\varepsilon_T \approx 2.5$, but these data are probably influenced by the energetic inhomogeneity (a predominant contribution to fluorescence of the highest-energy states [35]).

We can conclude that the two-step charge separation can, under defined conditions, proceed practically activationlessly, and, hence, compete effectively with a one-step activationless reaction. The possibility cannot be excluded that, in different organisms, the energy of the intermediate varies due, for example, to variation of the BChl's protein surroundings. Therefore, the auxiliary BChl can play, in principle, different roles.

4. Pheophytin-quinone electron transfer

In this case, ΔG depends not on the sum but on the difference of charging energies, and does not include the Coulombic interaction between reaction partners. Hence, the expressions for ΔG and E_s for this reaction have a different form, and we cannot expect an automatic compensation of effects of ε_T on these two quantities. As the reaction takes place before neutralization of the special pair, we have to take into account the interaction of the negative charge on BPh or Q with the positive charge of P.

The charging of P takes few picoseconds, and hence the time-evolution of the dielectric response to this charge proceeds practically simultaneously with the response to the charge transfer from BPh^- to Q_A, having a characteristic duration of few hundreds of picoseconds. Therefore, in our description of the process, we can use the same effective ε_T for both charging of BPh and Q_A and the interaction of these charges with P^+.

The effective dielectric constant at times of few picoseconds was estimated in the previous section as about 2.9, at nanoseconds $\varepsilon_T \sim 3.3$; hence for the process under consideration having a characteristic time of a hundred picoseconds, the value of $\varepsilon_T \sim 3.0$ to 3.1 could be accepted.

Let us estimate the value of ΔG for this charge shift reaction, ΔG_{sh}. The data on delayed fluorescence from the state $P^+ Q_A^-$ (in RC of *Rb. sphaeroides*, the characteristic time 0.1 s) give this state lying by 0.86 eV lower by free energy than P^* [27,44]. Subtracting the $\Delta G_{cs}^o = -0.30$ to -0.32 eV estimated above, we obtain $\Delta G_{sh}^o = -0.56$ to -0.54 eV. However, this value cannot be considered as corresponding exactly to the energy level stabilized by the dielectric relaxation only, but includes some additional stabilization with a characteristic time of hundreds of microseconds [45,46]. This is probably due to protonation of some side-chains. In the fast electron transfer, the protonation does not take place, and hence its effect should not be included in the standard value of ΔG_{sh}^o appropriate to the analysis of the process. Using the data [47] on the pH dependence of ΔG^o for the $P^+ Q_A^-$ recombination, the corresponding correction was estimated as being less than $+0.03$ eV [12], and hence a reasonable estimate of ΔG_{sh}^o is about -0.52 to -0.54 eV.

For an analysis of the process in the time interval of order of hundreds of picoseconds, we need to introduce a correction to ΔG_{sh} due to the difference in solvation energies of ions in the multilayer membrane at $\varepsilon_s = 4$ and $\varepsilon_T = 3$ to 3.1. The correction calculated with the membrane parameters given above results in $\Delta G_{sh} \approx -0.46$ to -0.48 eV and $\Delta G_{sh} \approx -0.49$ to -0.51 eV for the distances to boundary equal to 0.3 and 0.2 nm, respectively. In the same model and with the same parameters the reorganization energy was calculated to be equal to 0.34–0.37 eV and 0.45–0.47 eV. Adding the inner-sphere component $E_r \approx 0.04$ eV, we obtain the corresponding activation energies $E^{\neq} = 1.5$–6.6 meV and $E^{\neq} = 0.0$–0.2 meV, i.e., values low enough to describe the process as a practically activationless one.

It is interesting to note that, in spite of the absence of a strict compensation of the effects of ε_T on ΔG and E_s, in this particular case the result is almost insensitive to the value of ε_T (e.g., for $\varepsilon_T = \varepsilon_s = 4$, $E^{\neq} = 0.4$–1.2 and 5.5–7.5 meV). This is due to an additional effect of Coulombic interaction with P^+ and a fortuitous combination of geometric parameters. Therefore, the main result of this section, namely the activationless behavior of the $BPh^- \rightarrow Q_A$ transfer, is practically insensitive to the choice of parameters.

The reorganization energy for this electron transfer is substantially higher than for the charge separation step: this is necessary to adjust to a larger energy gap. I believe that this adjustment has been achieved by Nature using a proper geometry of the system, first of all a smaller effective radius of the electron acceptor [22].

For the $BPh^- \rightarrow Q$ reaction, there are in the literature some microscopic simulations [36,48]. Both of them, in concordance with semi-continuum results, give the reorganization energy practically 2-times higher than for the charge separation.

5. Charge recombination

For these reactions, the compensation of ε_T-dependent components of ΔG and E_s is also absent.

Let us consider first the recombination of P^+ and BPh^-. The reorganization energy for this process is the same as for charge separation (Fig. 1). The characteristic duration lies in bounds of tens of nanoseconds, hence the effective $\varepsilon_T \approx 3.3$ to 3.4. From the energy difference between the ground and excited states of P equal to 1.38 eV [26,44] and $\Delta G_{cs} = -0.30$ eV, we find for this recombination $\Delta G^o = -1.08$ eV; correction for transition from $\varepsilon_T = 4$ to $\varepsilon_T = 3.3$ to 3.4 (see Fig. 1) gives $\Delta G = -1.14 \pm 0.02$ eV. Comparison with $E_s = 0.25 \pm 0.01$ eV shows that the reaction lies far in the inverted region, and hence its activation energy should be very high (0.7 to 0.9 eV). As is usual for reactions in the inverted region [49], this makes more probable the formation of the reaction product in a vibrationally-excited state. As a result, the effective activation energy decreases substantially but the reaction rate decreases due to a low pre-exponential factor. Some examples of such behavior in homogeneous reactions are given in [50,51]. For the $P^+ - BPh^-$ recombination, relatively large reaction times at low activation energy were observed [52]. The inverted-region regime renders this recombination process unable to compete effectively with the forward electron transfer to Q_A.

The other pathway for P^+ BPh^- recombination is the rephasing to a triplet state with a subsequent recombination into a neutral triplet. The characteristic time of reaction is 2 ns [52]; hence, the effective $\varepsilon_T \approx 3.2$; the energy gap obtained from experiments in the 100 μs interval ($\varepsilon_T \approx 3.6$) is 0.17 eV [30,53], corrected for the change of ε_T $\Delta G = -0.21$ eV. The calculated values are: $E_s = 0.22$ eV, $E^{\neq} \approx 0.1$ meV. The process is revealed to be activationless, in agreement with experiment.

The last recombination path that will be considered here is the slow (≈ 0.1 s) recombination of P^+ and Q_A^- [27,31,44,54]. For this reaction, $\Delta G^\circ = 1.38 - 0.86 = 0.52$ eV. The reorganization energy (at $\varepsilon_s = 4$ and the distance of Q_A to the boundary equal to 0.3 nm) has been calculated as 0.68 eV. Adding $E_i \approx 0.04$ eV, we obtain $E^{\neq} = 14$ meV: the situation close to an activationless process.

6. Conclusions

In this paper, I present a more rigorous quantitative analysis of the problem posed in my previous study [12]. In the case of fast electron transfer reactions, we have to take into account that the protein's dielectric response evolves with time. Therefore, at short time intervals, not all the kinds of medium inertial polarization can manifest themselves, and, correspondingly, affect the charge transfer energetics. I describe this situation in terms of a set of effective dielectric constants ε_T corresponding to various time intervals.

It was shown that, for a charge separation process, the effects of the variable ε_T on both the reaction free energy and the reorganization energy are equal and opposite in sign, the result being correct for any homogeneous and heterogeneous dielectric medium. Therefore, these two effects are mutually compensating, and the process remains activationless, irrespective of the varying value of ε_T.

On the basis of the experimental data on the energy gaps corresponding to different time spans, the effective dielectric constants could be evaluated. They vary substantially in time starting with the value of about 2.9 at few picoseconds, through $\varepsilon_T \approx 3.3$ at 10 ns and ≈ 3.5 at 100 μs, to a static value of 4. With these parameters, the activation energies close to zero were calculated for some other reactions in RC, viz. for electron transfer from BPh^- to Q_A, for charge recombination in the radical pair P^+ BPh^- with formation of a triplet special pair ^3P, and for the $P^+Q_A^-$ recombination. It was found that the estimates of the temporal variation of the effective dielectric constant based on the data for one reaction provide a reasonable description for the other. Further, the results described above are only slightly sensitive to variation, within the reasonable bounds, of the model parameters. Therefore, we can consider the characteristics of the time-evolution of the effective dielectric constant obtained in this study to be reflecting the real trends.

Acknowledgements

The research described in this publication was made possible in part by Grant No. MD9000 from the International Science Foundation.

Appendix A. Comparison of ε_T effects on ΔG_{el} and E_s

The effective dielectric constant, ε_T, influences the charging energies of ions and the energy of their electrostatic interaction. This can be expressed as the difference in total energies of the electric field in the initial and final states

$$\Delta G_{el} = \frac{1}{8\pi}\int_V \frac{1}{\varepsilon_T}\left(\mathbf{D}_f^{s2} - \mathbf{D}_i^{s2}\right)dv \tag{AI.1}$$

where ε_T represents the time-dependent effective value of the static dielectric constant ε_s.

The corresponding component of E_s (which will be designated E_s^s) is expressed by the second term of Eq. (2).

Let us consider the transfer of a charge qe between two particles with initial charges me and ne. Introducing two 'geometric' functions, f_m and f_n, and taking into account proportionality of the electric field to the charge creating this field, we can write

$$\mathbf{D}_i^s = e(f_m m + f_n n) \tag{AI.2}$$

$$\mathbf{D}_f^s = e(f_m m + f_n n + f_m q - f_n q) \tag{AI.3}$$

Substituting (AI.2) and (AI.3) into Eqs. (2) and (AI.1) we obtain

$$\Delta G_{el} = \frac{e^2}{8\pi}\int_V \frac{1}{\varepsilon_T}\left[2(f_m m + f_n n)(f_m - f_n)q + (f_m - f_n)^2 q^2\right]dv \tag{AI.4}$$

$$E_s^s = -\frac{e^2}{8\pi}\int_V \frac{1}{\varepsilon_t}(f_m - f_n)^2 q^2 dv \tag{AI.5}$$

The field set up by two charges situated in different points is, generally, different, i.e., $f_m \neq f_n$. Therefore, $\Delta G_{el} = -E_s^s$ only in the case of $m = n = 0$, i.e., only for the charge separation between two initially neutral particles. For any other process, the sum $\Delta G_{el} + E_s^s \neq 0$ and depends on ε_T.

The above consideration gives a visual proof that E_s^* is nothing else than the charging energy of two ions with charges $+qe$ and $-qe$ in the medium with static dielectric constant ε_s (the term 'charging energy' is used here in a generalized sense, as the energy of charging of two ions situated in definite positions at a finite distance between them; this energy equals the energy of charging of separate ions plus the energy of their interaction). The first term in Eq. (2) presents the same, but in a medium with optical constant ε_0. The medium reorganization energy, E_s, is the difference of generalized charging energies in 'optical' and 'static' media.

This conclusion is true only for the correct, i.e., 'fixed-charge' formalism, resulting in Eq. (2). The 'fixed-displacement' approach gives a different formula (AI.6) which cannot be represented as a difference of corresponding charging energies:

$$E_s + \frac{1}{8\pi}\int_V \left(\frac{1}{\varepsilon_0} - \frac{1}{\varepsilon_s}\right)(\mathbf{D}_f^s - \mathbf{D}_i^s)^2 \mathrm{d}v \qquad \text{(AI.6)}$$

In implementing calculations for various systems, it is convenient to proceed from integration of $\mathbf{D}^2$ over volume to integration of $\varepsilon^2\varphi\nabla\varphi$ (φ is potential) over all surfaces of the charge-free dielectric phases, that means over the outer surfaces of ions and over both sides of all other boundaries. With Eq. (2), the last integrals are equal and opposite in sign, so they cancel each other, and only integrals over ions' surfaces remain. The latter are nothing else than charging energy. On the contrary, the integrals corresponding to (AI.6) do not cancel, and the final result takes on a more complex (and incorrect) form (for a more detailed discussion of surface integrals see, for example, [13])

Appendix B. The medium reorganization energy for the three-layer model of membrane

Let us consider the model depicted in Fig. 2: a core slab of thickness H with dielectric constant ε_1, two interlayers with the corresponding parameters h and ε_2, and two semi-infinite phases with ε_3 (water). Reactants 1 and 2 are situated inside the core at distances $l_1(l_2)$ from its left and r_1 (r_2) from the right boundary. The distance between two normals drawn through the centers of ions is d.

The solution to this electrostatic problem was given in [13] as the direct Coulombic field of ion plus the field of several infinite series of images. An example of the first images of ion 1 is shown in Fig. 2 (marked by a cross). The distance of any point from the left image is designated as $R'(l)$: this means the distance from the point situated at l_1 to left from the left boundary between phases I and II. For instance, this distance to the center of ion 1 equals $2l_1$, to the ion 2 it is $[(l_1+l_2)^2+d^2]^{1/2}$. Similarly, the distances from the point right to this boundary are designated as $R(l)$, left or right to the right boundary as $R^*(r)$ and $R''(r)$, respectively (see Fig. 2).

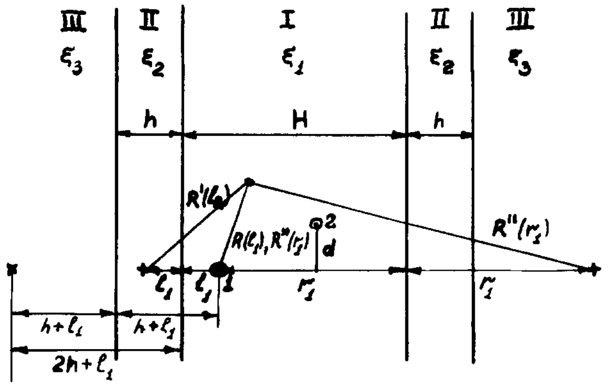

Fig. 2. Three-layer model of membrane. Phase I – inner core, II – interlayer, III – aqueous solution. H is the thickness of the core, h that of interlayer. Reactants 1 and 2 are designated by a dot in a circle, + is the charge's first image, × is one of the second images, ● is an arbitrary point inside the core.

The final expression for the potential in phase I is

$$\varphi = \frac{e}{\varepsilon_1 R(l)} + \varphi'(l) + \varphi'(r) + \varphi''(l) + \varphi''(r) \qquad \text{(AII.1)}$$

Here $\varphi'(l)$, $\varphi'(r)$ are the potentials set up by the left and right images if we consider only the left or right boundaries; an additional contribution $\varphi''(l)$, $\varphi''(r)$ arises due to reflection of left images at the right boundaries and vice versa. The expressions for these image potentials are

$$\varphi'(l)\frac{\varepsilon_1}{e} = \frac{K_1}{R'(l)} + L_1L_2K_2\sum_{n=0}^{\infty}\frac{(-K_1K_2)^n}{R'[2(n+1)h+l]} \qquad \text{(AII.1a)}$$

$$\begin{aligned}\varphi''(l)\frac{\varepsilon_1}{e} = {} & \frac{K_1^2}{R(2H+l)} + L_1L_2K_1K_2 \\ & \times\left\{\sum_{n=0}^{\infty}\frac{(-K_1K_2)^n}{R[2(n+1)h+2h+l]} \right. \\ & \left. + \frac{1}{R[2H+2h+l]}\right\} \\ & + L_1^2L_2^2K_2^2\sum_{n=0}^{\infty}\frac{(-K_1K_2)^n}{R[2(n+2)h+2H+l]} \\ & + \frac{K_1^3}{R'[2H+l]} + L_1L_2K_1^2K_2 \\ & \times\left\{\sum_{n=0}^{\infty}\frac{(-K_1K_2)^n}{R'[2(n+1)h+2H+l]} \right. \\ & \left. + \frac{2}{R'[2H+2h+l]}\right\}\end{aligned}$$

$$+\frac{L_1K_1^2K_2}{R'[2H+2h+l]}+L_1^2L_2^2K_1K_1^2\times\left\{2\sum_{n=0}^{\infty}\frac{(-K_1K_2)^n}{R'[2(n+2)h+2H+l]}+\frac{1}{R'[2H+4h+l]}\right\}+L_1^2L_2^3K_2^3\sum_{n=0}^{\infty}\frac{(-K_1K_2)^n}{R'[2(n+3)h+2H+l]} \qquad \text{(AII.1b)}$$

The expressions for $\varphi'(r)$ and $\varphi'(r)$ can be easily obtained from (AII.1a,b) by the following substitutions: $l \Rightarrow r$, $R' \Rightarrow R''$, $R^* \Rightarrow R$. The additional designations in Eqs. (AII.1a, AII.1b) are: $K_1=(\varepsilon_1-\varepsilon_2)/(\varepsilon_1+\varepsilon_2)$, $K_2=(\varepsilon_2-\varepsilon_3)/(\varepsilon_2+\varepsilon_3)$, $L_1=2\varepsilon_1/(\varepsilon_1+\varepsilon_2)$, $L_2=2\varepsilon_2/(\varepsilon_1+\varepsilon_2)$.

Bearing in mind that H is several-fold greater than h, I have restricted the series only with the terms in denominator involving H with a coefficient ≤ 4.

With the potential (AII.1), we have found the charging energies A; these energies should be calculated in optical and static media (constants $\varepsilon_{\mathrm{oi}}$ and $\varepsilon_{\mathrm{si}}$, and corresponding L_i, K_i), and, further, the reorganization energy can be found, as follows from Eq. (2), as their difference:

$$E_s=A^{\mathrm{o}}-A^{\mathrm{s}} \qquad \text{(AII.2)}$$

$$A\frac{\varepsilon_i}{e^2}=\frac{1}{2a_1}+\frac{1}{2a_2}-\frac{1}{R}+K_1\left[\frac{1}{4l_1}+\frac{1}{4l_2}+\frac{1}{4r_1}+\frac{1}{4r_2}-\frac{1}{\sqrt{d^2+(l_1+l_2)^2}}-\frac{1}{\sqrt{d^2+(r_1+r_2)^2}}\right]$$
$$+\frac{L_1L_2K_2}{4}\sum_{n=0}^{\infty}(-K_1K_2)^n\left[\frac{1}{(n+1)h+l_1}+\frac{1}{(n+1)h+l_2}-\frac{4}{\sqrt{d^2+[2(n+1)h+l_1+l_2]^2}}+\frac{1}{(n+1)h+r_1}+\frac{1}{(n+1)h+r_2}-\frac{4}{\sqrt{d^2+[2(n+1)h+r_1+r_2]^2}}\right]$$
$$K_1^2\left[\frac{1}{H}-\frac{1}{\sqrt{d^2+(H+l_1+r_2)^2}}-\frac{1}{\sqrt{d^2+(H+l_2+r_1)^2}}\right]$$
$$+L_1L_2K_1K_2\sum_{n=0}^{\infty}(-K_1K_2)^n\left[\frac{1}{(n+1)h+H}-\frac{1}{\sqrt{d^2+[2(n+1)h+H+l_1+r_2]^2}}-\frac{1}{\sqrt{d^2+[2(n+1)h+H+l_2+r_1]^2}}\right]$$
$$+L_1L_2K_1K_2\left[\frac{1}{H+h}-\frac{1}{\sqrt{d^2+(H+2h+l_1+r_2)^2}}-\frac{1}{\sqrt{d^2+(H+2h+l_2+r_1)^2}}\right]$$
$$+L_1^2L_2^2K_2^2\sum_{n=0}^{\infty}(-K_1K_2)^n\left[\frac{1}{(n+2)h+H}-\frac{1}{\sqrt{d^2+[2(n+2)h+H+l_1+r_2]^2}}-\frac{1}{\sqrt{d^2+[2(n+2)h+H+l_2+r_1]^2}}\right]$$
$$+\frac{K_1^3}{4}\left[\frac{1}{H+l_1}+\frac{1}{H+l_2}+\frac{1}{H+r_1}+\frac{1}{H+r_2}-\frac{4}{\sqrt{d^2+(2H+l_1+l_2)^2}}-\frac{4}{\sqrt{d^2+(2H+r_1+r_2)^2}}\right]$$
$$+L_1L_2K_1^2K_2\sum_{n=0}^{\infty}(-K_1K_2)^n\times\left[\frac{1}{(n+1)h+H+l_1}+\frac{1}{(n+1)h+H+l_2}+\frac{1}{(n+1)h+H+r_1}+\frac{1}{(n+1)h+H+r_2}-\frac{4}{\sqrt{d^2+[2(n+1)h+H+l_1+l_2]^2}}-\frac{4}{\sqrt{d^2+[2(n+1)h+H+r_1+r_2]^2}}\right]$$

$$
+2L_1L_2K_1^2K_2\left[\frac{1}{4(H+h+l_1)}+\frac{1}{4(H+h+l_2)}\right.
$$

$$
+\frac{1}{4(H+h+r_1)}+\frac{1}{4(H+h+r_2)}
$$

$$
-\frac{1}{\sqrt{d^2+(2H+2h+l_1+l_2)^2}}
$$

$$
\left.-\frac{1}{\sqrt{d^2+(2H+2h+r_1+r_2)^2}}\right]
$$

$$
+\frac{L_1^2L_2^2K_1K_2^2}{2}\sum_{n=0}^{\infty}(-K_1K_2)^n\left[\frac{1}{(n+2)h+H+l_1}\right.
$$

$$
+\frac{1}{(n+2)h+H+l_2}+\frac{1}{(n+2)h+H+r_1}
$$

$$
+\frac{1}{(n+2)h+H+r_2}
$$

$$
-\frac{4}{\sqrt{d^2+[2(n+2)h+2H+l_1+l_2]^2}}
$$

$$
\left.-\frac{4}{\sqrt{d^2+[2(n+2)h+2H+r_1+r_2]^2}}\right]
$$

$$
+\frac{L_1^2L_2^2K_1K_2^2}{4}\left[\frac{1}{H+2h+l_1}+\frac{1}{H+2h+l_2}\right.
$$

$$
+\frac{1}{H+2h+r_1}+\frac{1}{H+2h+r_2}
$$

$$
-\frac{4}{\sqrt{d^2+(2H+4h+l_1+l_2)^2}}
$$

$$
\left.-\frac{4}{\sqrt{d^2+(2H+4h+r_1+r_2)^2}}\right]+\frac{L_1^3L_2^2K_2^3}{4}
$$

$$
\times\sum_{n=0}^{\infty}(-K_1K_2)^n\left[\frac{1}{(n+3)h+H+l_1}\right.
$$

$$
+\frac{1}{(n+3)h+H+l_2}+\frac{1}{(n+3)h+H+r_1}
$$

$$
+\frac{1}{(n+3)h+H+r_2}
$$

$$
-\frac{4}{\sqrt{d^2+[2(n+3)h+2H+l_1+l_2]^2}}
$$

$$
\left.-\frac{4}{\sqrt{d^2+[2(n+3)h+2H+r_1+r_2]^2}}\right] \tag{AII.3}
$$

This equation looks rather cumbersome; however, it is quite easy to compute according to (AII.3), because all series converge quite rapidly.

It is easy to see that, for an infinite homogeneous dielectric ($\varepsilon_1 = \varepsilon_2 = \varepsilon_3$ or/and $l_i = r_i = H = h = \infty$), Eqs. (AII.2 and 3) transform into the usual Marcus equation

$$
E_s = e^2\left(\frac{1}{\varepsilon_o}-\frac{1}{\varepsilon_s}\right)\left(\frac{1}{2a_1}+\frac{1}{2a_2}-\frac{1}{R}\right) \tag{AII.4}
$$

Appendix C. The geometric parameters of the RC model

On the basis of X-ray data on homologous structures of *Rps. viridis* and *Rb. sphaeroides* (see, for example, [55,56]), I accepted the RC membrane thickness of 5.0 to 5.4 nm with inner core 3.3 to 3.6 nm thick and intermediate layers (containing practically all X-ray-visible water) at each side of membrane 0.8 to 1.0 nm thick. Variations in thicknesses in these limits (at other parameters kept constant) do not change E_s substantially (in range of 3 to 4 meV).

For the position of the boundary separating the inner core and the outer layer of membrane, I have chosen the plane separating hydrophobic and hydrophilic side-chains of the outer segments of L and M subunits: more precisely, the middle of the α-helices Lcd and Mcd (and Le, Me) covering the special pair. The distance from the special pair center and this boundary is about 0.5 nm. The influence of its variations is shown in Fig. 1.

At the other side of membrane, the closest to its boundary are quinones. According to structural data [57], Q_A touches mainly the hydrophobic residues but the nearby Q_B has many hydrophilic residues in its environment, and, moreover, one can discern near it a void filled, probably, with mobile water molecules [58]. Hence, I draw the inner-core boundary not far from the Q_A center but at the distance of 0.3 nm, i.e., practically at the van der Waals contact with this molecule. Other positions of the boundary were also tried, in particular the distance of 0.2 nm intended to mimic the effect of a closer approach of the high-dielectric medium.

Eqs. (AII. 3) as well as the Marcus equation relate to spherical reactants. The redox-components of RC are closer to strongly oblate spheroids. The formulae for the reactants of the kind were obtained in [59]. They can be presented in the form similar to (AII.4) using some effective radii; an estimate of the latter is given in [22]. Some approximations concerning the effect of the spheroids mutual orientation have been also discussed there. Another approximation implied in Eq. (AII.4) is the neglect of the effects of the field distortion by the second reactant and of its volume exclusion [60]. However, these effects decrease rapidly with the increasing inter-reactant distance. In the present case, for most redox couples, this distance exceeds markedly the sum of reactants' radii, and therefore the corresponding correction should be really small. The field-distortion effect should be also small because of rather close (and low) values of the effective ε values of the reactants and their proteinaceous surroundings.

References

[1] Parson, W.W. and Ke, B. (1982) in Photosynthesis (Govindjee, ed.), Vol. 1, pp. 331–385, Academic Press, New York.

[2] Jortner, J. (1980) Biochim. Biophys. Acta 594, 193–230.

[3] Marcus, R.A. and Sutin, N. (1985) Biochim. Biophys. Acta 811, 265–322.

[4] Kirmaier, C. and Holten, D. (1987) Photosynth. Res. 13, 225–260.

[5] Krishtalik, L.I. (1986) Charge Transfer Reactions in Electrochemical and Chemical Processes, Ch. 7, Plenum Press, New York.

[6] Krishtalik, L.I. (1988) in The Chemical Physics of Solvation (Dogonadze, R.R., Kálmán, E., Kornyshev, A.A. and Ulstrup, J., eds.), Part C, pp. 707–739, Elsevier, Amsterdam.

[7] Krishtalik, L.I. (1988) J. Mol. Catal. 47, 211–218.

[8] Gurd, F.R.N. and Rothgeb, T.M. (1979) Adv. Prot. Chem. 33, 74–165.

[9] Karplus, M. and McCammon, J.A. (1991) CRC Crit. Rev. Biochem. 9, 293–349.

[10] Frauenfelder, H., Sligar, S.G. and Wolynes, P.G. (1991) Science 254, 1598–1603.

[11] Brooks III, C.L., Karplus, M. and Pettitt, B.M. (1988) Proteins, A Theoretical Perspective of Dynamics, Structure, and Thermodynamics, Wiley, New York.

[12] Krishtalik, L.I. (1995) Biochim. Biophys. Acta 1228, 58–66.

[13] Krishtalik, L.I. (1992) Molekul. Biologiya 26, 1377–1388.

[14] Liu, Y.-P. and Newton, M.D. (1994) J. Phys. Chem. 98, 7162–7169.

[15] Marcus, R.A. (1994) J. Phys. Chem. 98, 7170–7174.

[16] Medvedev, I.G. and Kuznetsov, A.M. (1995) Elektrokhimiya, in press.

[17] Cherepanov, D.A. and Krishtalik, L.I. (1990) Bioelectrochem. Bioenerg. 24, 113–127.

[18] Calef, D.F. and Wolynes, P.G. (1983) J. Phys. Chem. 87, 3387–3400.

[19] Xu, D. and Schulten, K. (1994) Chem. Phys. 182, 91–117.

[20] Warshel, A. (1980) Proc. Natl. Acad. Sci. USA 77, 3105–3109.

[21] Grampp, G. and Jaenicke, W. (1984) Ber. Bunsenges. Phys. Chem. 88, 325–334.

[22] Krishtalik, L.I. (1989) Biochim. Biophys. Acta 977, 200–206.

[23] Dracheva, S.M., Drachev, L.A., Konstantinov, A.A., Semenov, A.Y., Skulachev, V.P., Arutjunjan, A.M., Shuvalov, V.A. and Zaberezhnaya, S.M. (1988) Eur. J. Biochem. 174, 253–264

[24] Vorotyntsev, M.A., Kuznetsov, A.M. and Dogonadze, R.R. (1970) Dokl. Akad. Nauk. SSSR 195, 113–115.

[25] Kuznetsov, A.M., Ulstrup, J. and Vorotyntsev, M.A. (1988) in The Chemical Physics of Solvation (Dogonadze, R.R., Kálmán, E., Kornyshev, A.A. and Ulstrup, J., eds.), Part C, pp. 163–273, Elsevier, Amsterdam.

[26] Woodbury, N.W.T. and Parson, W.W. (1984) Biochim. Biophys. Acta 767, 345–361.

[27] Woodbury, N.W.T., Parson, W.W., Gunner, M.R., Prince, R.C. and Dutton, P.L. (1986) Biochim. Biophys. Acta 851, 6–22.

[28] Peloquin, J.M., Williams, J.C., Lin, X., Alden, R.G., Taguchi, A.K.W., Allen, J.P. and Woodbury, N.W. (1994) Biochemistry 33, 8089–8100.

[29] Woodbury, N.W., Peloquin, J.M., Alden, R.G., Lin, X., Lin, S., Taguchi, A.K.W., Williams, J.C. and Allen, J.P. (1994) Biochemistry 33, 8101–8112.

[30] Goldstein, R.A., Takiff, L. and Boxer, S.G. (1988) Biochim. Biophys. Acta 934,253–263.

[31] Shopes, R.J. and Wraight, C.A. (1987) Biochim. Biophys. Acta 899, 409–425.

[32] Franzen, S. and Boxer, S.G. (1993) J. Phys. Chem. 97, 6304–6318.

[33] Bixon, M. and Jortner, J. (1986) J. Phys. Chem. 90, 3795–3800.

[34] Pierce, D.W. and Boxer, S.G. (1992) J. Phys. Chem. 96, 5560–5566.

[35] Ogrodnik, A., Keupp, W., Volk, M., Aumeier, G. and Michel-Beyerle, M.E. (1994) J. Phys. Chem. 98, 3432–3439.

[36] Schulten, K. and Tesch, M. (1991) Chem. Phys. 158,421–446.

[37] Treutlein, M., Schulten, K., Brünger, A.T., Karplus, M., Deisenhofer, J. and Michel, H. (1992) Proc. Natl. Acad. Sci. USA 89, 75–79.

[38] Creighton, S., Hwang, J.K., Warshel, A., Parson, W.W. and Norris, J. (1988) Biochemistry 27, 774–781.

[39] Parson, W.W., Chu, Z.-T. and Warshel, A. (1990) Biochim. Biophys. Acta 1017, 251–272.

[40] Marchi, M., Gehlen, J.N., Chandler, D. and Newton, M. (1993) J. Am. Chem. Soc. 115, 4178–4190.

[41] Shuvalov, V.A. and Klimov, V.V. (1987) Biofizika 32, 814–829.

[42] Holzapfel, W., Finkele, U., Kaiser, W. Oesterhelt, D., Scheer, H., Stilz, H.U. and Zinth, W. (1990) Proc. Natl. Acad. Sci. USA 87, 5168–5172.

[43] Bixon, M., Jortner, J., Michel-Beyerle, M.E., Ogrodnik, A. and Lersch, W. (1987) Chem. Phys. Lett. 140, 626–630.

[44] Arata, H. and Parson, W.W. (1981) Biochim. Biophys. Acta 638, 201–209.

[45] Brzezinski, P., Okamura, M.Y. and Feher, G. (1992) in The Photosynthetic Bacterial Reaction Center II (Breton, J. and Verméglio, A., eds.), pp. 321–330, Plenum Press, New York.

[46] Tiede, D.M. and Hanson, D.K. (1992) in The Photosynthetic Bacterial Reaction Center II (Breton, J. and Verméglio, A., eds.), pp. 341–350, Plenum Press, New York.

[47] McPherson, P.H., Nagarajan, V., Parson, W.W., Okamura, M.Y. and Feher, G. (1990) Biochim. Biophys. Acta 1019, 91–94.

[48] Warshel, A., Chu, Z.-T. and Parson, W.W. (1989) Science 246, 112–116.

[49] Dogonadze, R.R., Kuznetsov, A.M. and Vorotyntsev, M.A. (1976) Zs. phys. Chem., N. F. 100, 1–16.

[50] Closs, G.L., Calcaterra, L.T., Green, N.J., Penfield, K.W. and Miller, J.R. (1986) J. Phys. Chem. 90, 3673–3643.

[51] Liang, N., Miller, J.R. and Closs, G.L. (1990) J. Am. Chem. Soc. 112, 5353–5354.

[52] Ogrodnik, A., Remy-Richter, N., Michel-Beyerle, M.E. and Feick, R. (1987) Chem. Phys. Lett. 135, 576–581.

[53] Takiff, L. and Boxer, S.G. (1988) Biochim. Biophys. Acta 932, 325–334.

[54] Gunner, M.R. and Dutton, P.L. (1989) J. Am. Chem. Soc. 111, 3400–3412.

[55] Deisenhofer, J. and Michel, H. (1989) EMBO J. 8, 219–2169.

[56] Allen, J.P., Feher, G., Yeates, T.O., Komiya, H. and Rees, D.C. (1987) Proc. Natl. Acad. Sci. USA 84, 6162–6166.

[57] Allen, J.P., Feher, G., Yeates, T.O., Komiya, H. and Rees, D.C. (1988) Proc. Natl. Acad. Sci. USA 85, 8487–8491.

[58] Beroza, P., Fredkin, D.R., Okamura, M.Y. and Feher, G. (1992) in The Photosynthetic Bacterial Reaction Center II (Breton, J. and Verméglio, A., eds.), pp. 363–373, Plenum Press, New York.

[59] Kharkats, Yu.I. (1976) Elektrokhimiya 12, 1284–1291.

[60] Kharkats, Yu.I. (1976) Elektrokhimiya 12, 592–594.